Numerical Simulation of Quantum Distributions: Instability and Quantum Chaos

G.Y. Kryuchkyan, H.H. Adamyan, and S.B. Manvelyan

Institute for Physical Research, National Academy of Sciences,
Ashtarak-2, 378410, Armenia
Yerevan State University, Alex Manookyan 1, 375049,
Yerevan, Armenia

Abstract. Quantum state diffusion with moving basis approach is formulated for computation of Wigner functions of open quantum systems. The method is applied to two quantum nonlinear dissipative systems. Quantum dynamical manifestation of chaotic behavior, including emergence of chaos, as well as the formation of Hopf bifurcation in quantum regime are studied by numerical simulation of ensemble averaged Wigner functions.

1 Introduction and Models

All real experiments in quantum physics always deal with open systems, which are not even approximately isolated and significantly affected by the environment. Interaction with the environment leads to dissipation and decoherence, i.e. to irreversible loss of energy and coherence, and can monitor some of the system observables. Decoherence can destroy the quantum-mechanical interference or quantum superposition of states. All quantum systems suffer from decoherence, but it has very specific implications in area of quantum information and quantum computation.

The present paper is devoted to the problem of numerical simulation of dissipation and decoherence in open quantum system. We concentrated mainly on investigation of so-called quantum chaotic systems - quantum systems, which have chaotic dynamic in a classical limit. Their analysis requires the high-performance calculations as well as the development of new numerical algorithms.

One of the most practical tools for analyzing the time-evolution of an open quantum system is the master equation for the density matrix. However, the analytical studies in this area are very difficult and the solutions of master equations have been established only for relatively simple models. We remind the reader of a common approach to analysis of an open system. The starting point is the master equation in Lindblad form [1] for reduced density matrix $\rho(t) = Tr(\rho_{tot}(t))$

V.N. Alexandrov et al. (Eds.): ICCS 2001, LNCS 2074, pp. 1041–1049, 2001.

which is obtained from the total density matrix of the universe by tracing over the environment Hilbert space

$$\frac{\partial \rho}{\partial t} = -\frac{i}{\hbar}\left[H,\rho\right] + \sum_i \left(L_i \rho L_i^+ - \frac{1}{2} L_i^+ L_i \rho - \frac{1}{2} \rho L_i^+ L_i \right). \tag{1}$$

Here H is the Hamiltonian of the system and L_i are Lindblad operators which represent the effect of the environment on the system in a Markov approximation. Numerically there is often a large advantage in representing a system by quantum state rather than a density matrix. On this direction, there are many ways to "unraveling" the master equation into "trajectories" [2]. Our numerical analysis is based on the quantum state diffusion (QSD) approach which represents the density matrix into component stochastic pure states $|\Psi_\xi(t)\rangle$ describing the time-evolution along a quantum trajectory [3]. According to QSD the reduced density operator is calculated as the ensemble mean $\rho(t) = M(|\Psi_\xi(t)\rangle \langle\Psi_\xi(t)|)$, with M denoting the ensemble average. The corresponding equation of motion is

$$\begin{aligned} |d\Psi_\xi\rangle = &-\frac{i}{\hbar} H |\Psi_\xi\rangle \, dt - \\ &\frac{1}{2} \sum_i \left(L_i^+ L_i - 2 \left\langle L_i^+ \right\rangle L_i + \langle L_i \rangle \left\langle L_i^+ \right\rangle \right) |\Psi_\xi\rangle \, dt + \sum_i \left(L_i - \langle L_i \rangle \right) |\Psi_\xi\rangle \, d\xi_i. \end{aligned} \tag{2}$$

Here ξ indicates the dependence on the stochastic process, the complex Wiener variables $d\xi_i$ satisfy the fundamental correlation properties:

$$M\left(d\xi_i\right) = 0, \; M\left(d\xi_i d\xi_j\right) = 0, \; M\left(d\xi_i d\xi_j^*\right) = \delta_{ij} dt, \tag{3}$$

and the expectation value equals $\langle L_i \rangle = \langle \Psi_\xi \left| L_i \right| \Psi_\xi \rangle$.

In what follows we apply this method for numerical calculations of quantum distributions averaged on trajectories. Among them the Wigner function play a central role because provides a wide amount of information about the system and also provides a pictorial view. Below we shall give the results of numerical calculations for two models of driven, dissipative nonlinear oscillators, which are relevant to some systems in quantum optics.

One of those is the model of nonlinear oscillator driven by two periodic forces, which described by the Hamiltonian

$$H = \hbar\omega_0 a^+ a + \hbar\chi (a^+ a)^2 + \hbar \left[\left(\Omega_1 \exp(-i\omega_1 t) + \Omega_2 \exp(-i\omega_2 t) \right) a^+ + h.c. \right], \tag{4}$$

where a, a^+ are boson annihilation and creation operators, ω_0 is an oscillatory frequency, ω_1 and ω_2 are the frequencies of driving fields, and χ is the strength

of the anharmonicity. The couplings with two driving forces are given by Rabi frequencies Ω_1 and Ω_2.

The other is the model of two driven harmonic oscillators coupled by a nonlinear process, which is described by the following Hamiltonian

$$H = \hbar\omega_1 a_1^+ a_1 + \hbar\omega_2 a_2^+ a_2 + i\hbar\left(Ee^{-i\omega t}a_1^+ - E^* e^{-i\omega t}a_1\right) + i\hbar\frac{k}{2}\left(a_1^{+2}a_2 - a_1^2 a_2^+\right). \tag{5}$$

Here a_1 , a_2 are the operators of the modes at the frequencies ω_1 and ω_2 respectively, k is the coupling coefficient between the modes , which in the case of an optical interaction can be proportional to the second-order nonlinear susceptibility $\chi^{(2)}$; E is a complex amplitude of the periodic force at the frequency ω.

2 MQSD Algorithm for Wigner Function

It seems naturally to use the Fock's state basis of two harmonic oscillators $\{|n\rangle_1 \otimes |m\rangle_2 ;\ n, m \in (0, 1, 2, ..., N)\}$ for numerical simulation. Unfortunately, in the most interesting cases, which are relevant to experiments, the effective number of Fock's states quickly becomes impractical. On this reason, it is very difficult to obtain a single quantum trajectory in such regimes, not to mention performing an ensemble averaging. However, it is possible to reduce significantly the number of need basis states by choosing an appropriate basis. It was demonstrated in Ref.[4] considering quantum state diffusion with moving basis (MQSD). Its advantages for computation was also shown in [4]. In this paper we develope the MQSD method for calculation of distribution functions including Wigner functions.

At first, we shortly describe the application of MQSD method for the numerical simulation of Wigner function using the standard definition based on the density matrix [2]. We have for each of the modes of the harmonic oscillators

$$W_i(\alpha) = \frac{1}{\pi^2}\int d^2\gamma Tr(\rho_i D(\gamma))\exp(\gamma^*\alpha - \gamma\alpha^*), \tag{6}$$

where the reduced density operators for each of the modes are constructed by tracing over the other mode

$$\rho_{1(2)} = Tr_{2(1)}(\rho), \qquad \rho = M(|\Psi_\xi\rangle\langle\Psi_\xi|). \tag{7}$$

We use the expansion of the state vector $|\Psi_\xi(t)\rangle$ in the basis of excited coherent states of two modes as

$$|\Psi_\xi(t)\rangle = \sum a_{nm}^{\xi}(\alpha_\xi, \beta_\xi)\,|\alpha_\xi, n\rangle_1\,|\beta_\xi, m\rangle_2\,, \tag{8}$$

where

$$|\alpha, n\rangle_1 = D_1(\alpha)\,|n\rangle_1\,, \quad |\beta, m\rangle_2 = D_2(\beta)\,|m\rangle_2 \tag{9}$$

are the excited coherent states centered on the complex amplitude $\alpha = \langle a_1 \rangle$, $\beta = \langle a_2 \rangle$. Here $|n\rangle_1$ and $|m\rangle_2$ are Fock's number states of the fundamental and second -harmonic modes, and D_1 and D_2 are the coherent states displacement operators

$$D_i(\alpha) = \exp(\alpha a_i^+ + \alpha^* a_i). \tag{10}$$

As it is known, the MQSD method is very effective for numerical simulation of quantum trajectories. However, the problem is that in this approach the two mode state vector $|\Psi_\xi(t)\rangle$ is expressed in the individual basis depending on the realization. It creates the additional definite difficulties for calculation of the density matrix at each time of interest on the formula (7), which contains the averaging on the ensemble of all possible states. In practical point of view, it is useful to operate with state vector $|\Psi_\xi(t)\rangle$ reduced to a basis which is the same for all realizations of the stochastic process $\xi(t)$. To avoid this we express the density operators as

$$\rho_i(t) = \sum_{nm} \rho_{nm}^{(i)}(t) \, |\sigma, n\rangle \, \langle \sigma, m| \tag{11}$$

in the basis of excited Fock states with an arbitrary coherent amplitude σ. It gives for the Wigner function (6)

$$W_i(\alpha + \sigma) = \sum_{nm} \rho_{nm}^{(i)} W_{nm}(r, \theta), \tag{12}$$

where (r, θ) are polar coordinates in the complex phase-space $X = Re\alpha = r\cos\theta$, $Y = Im\alpha = r\sin\theta$ and the coefficients W_{nm} are

$$W_{mn}(r,\theta) = \left\{ \begin{array}{l} \frac{2}{\pi}(-1)^n \sqrt{\frac{n!}{m!}} e^{i(m-n)\theta} (2r)^{m-n} e^{-2r^2} L_n^{m-n}(4r^2), \; m \geq n \\ \frac{2}{\pi}(-1)^m \sqrt{\frac{m!}{n!}} e^{i(m-n)\theta} (2r)^{n-m} e^{-2r^2} L_m^{n-m}(4r^2), \; n \geq m \end{array} \right\}, \tag{13}$$

where L_m^{n-m} are Laguerre polynomials.

As to the density matrix elements, they equal to

$$\rho_{nm}^{(1)}(\sigma_1) = M \left\{ \sum \langle n| \, D_1(\alpha_\xi - \sigma_1) \, |q\rangle \, \langle k| \, D_1^+(\alpha_\xi - \sigma_1) \, |m\rangle \, a_{qp}^{(\xi)}(\alpha_\xi, \beta_\xi) a_{kp}^{(\xi)*}(\alpha_\xi, \beta_\xi) \right\}, \tag{14}$$

$$\rho_{nm}^{(2)}(\sigma_2) = M \left\{ \sum \langle n| \, D_2(\beta_\xi - \sigma_2) \, |q\rangle \, \langle k| \, D_2^+(\beta_\xi - \sigma_2) \, |m\rangle \, a_{pq}^{(\xi)}(\alpha_\xi, \beta_\xi) a_{pk}^{(\xi)*}(\alpha_\xi, \beta_\xi) \right\}. \tag{15}$$

In short, the MQSD algorithm for numerical simulation is the following. In the initial basis centered at $\alpha = \beta = 0$ each set of stochastic $d\xi_i$ determines a quantum trajectory through Eqs.(2),(3).Then the state vectors (8) are calculated using a moving basis.

3 Pictorial View of Hopf Bifurcation

Now we apply the above numerical algorithm to calculate the ensemble-averaged Wigner function for the system of nonlinearly coupled, driven oscillators in contact with its environment. This model is accessible for experiments and is realized at least in the second-harmonic generation (SHG) in an optical cavity [5]. Intracavity SHG consists in transformation, via a $\chi^{(2)}$ nonlinear crystal, of an externally driven fundamental mode with the frequency ω_1 into the second-harmonic mode with the frequency $\omega_2 = 2\omega_1$ ($\omega_1 + \omega_2 \rightarrow \omega_2$). The system is described by both the Hamiltonians (5), and the Eqs.(1), (2). The Lindblad operators are $L_i = \sqrt{\gamma_i} a_i$, $(i = 1, 2)$, and γ_1, γ_2 are the cavity damping rates.

In the classical limit, this system is characterized by Hopf bifurcation which connect a steady-state regime to a temporal periodic regime (so-called self-pulsing instability [6]). In quantum treatment all quantum-mechanical ensemble-averaged quantities reach stable constant values at an arbitrary time exceeding the transient time. Therefore, the question has been posed what is the quantum-mechanical counerpart of a classical instability. The Wigner functions for the fundamental and second-harmonic modes have been analyzed in the vicinity of the Hopf bifurcation in Ref. [7], where it was shown that they describe "quantum instability". In this paper we expand our results [7] on the above Hopf-bifurcation range using MQSD algorithm. Below Hopf bifurcation the Wigner functions of both modes are Gaussian in the phase-space plane centered at $x = y = 0$. With increasing E we enter into critical transition domain, in the vicinity of Hopf bifurcation, where a spontaneous breaking of the phase symmetry occurs. The Wigner functions above bifurcation point at $E/E_{cr} = 2$ averaged over 1000 quantum trajectories are shown in Fig.1.

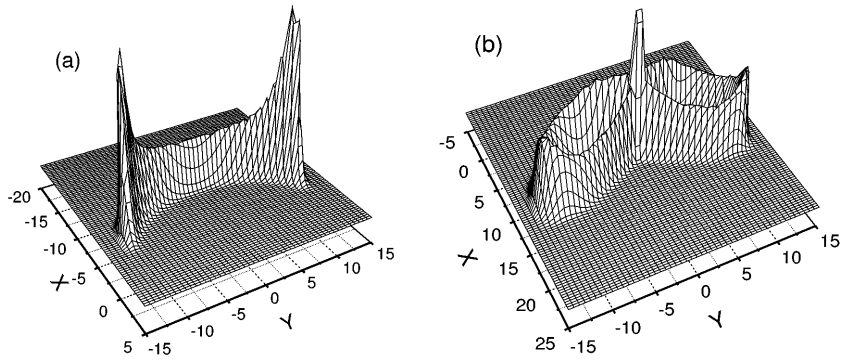

Fig. 1. The Wigner functions of the second-harmonic mode (a) and the fundamental mode (b) beyond the Hopf bifurcation for the parameters: $\gamma_1 = \gamma_2 = \gamma$, $k/\gamma = 0.3$, $E_{cr}/\gamma = 20$.

It is obvious, that the appearance of two side humps of Wigner functions correspond to two most probable values of phases. Generally speaking, the contour pots in (x, y) plane of the Wigner functions correspond to phase trajectories of the system in the classical limit. We show these results on Fig.2.

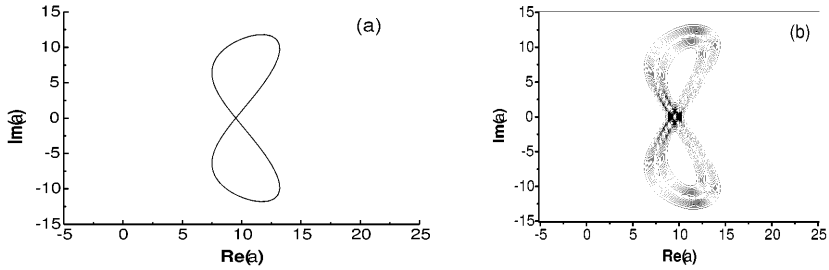

Fig. 2. Phase-space trajectory (a) and contour plot of Wigner function (b) for the fundamental mode.

4 Quantum Chaos on Wigner Functions

Our second example is the model of dissipative nonlinear oscillator driven by two periodic forces of different frequencies and interacting with heat bath. This model presents an example of open time-dependent quantum system showing dissipative chaos in classical limit. The model was proposed to study quantum stochastic resonance in the authors' previous paper [8], where it is shown, in particular, that the model is available for experiments. It is described by Hamiltonian (4) and Eqs. (1), (2), with the Lindblad operators $L_1 = \sqrt{(N+1)\,\gamma}a$, $L_2 = \sqrt{N\gamma}a^+$, where γ is the spontaneous decay rate and N denotes the mean number of quanta of a heat bath. For $\Omega_2 = 0$ this system is reduced to a single driven dissipative anharmonic oscillator which is a well known model in nonlinear physics (see Ref. [9] and [8] for full list of references). In the classical limit the considered double driven oscillator exhibits regions of regular and chaotic motion. Indeed, our numerical analysis of the classical equations of motion in the phase-space shows that classical dynamics of the system is regular in domains $\delta \ll \gamma$ and $\delta \gg \gamma$, where $\delta = \omega_2 - \omega_1$, and also when $\Omega_1 \ll \Omega_2$ or $\Omega_2 \ll \Omega_1$. The dynamics is chaotic in the range of parameters $\delta \sim \gamma$ and $\Omega_1 \simeq \Omega_2$.

Now we come to the question of what is the quantum manifestation of a classical chaotic dynamics on Wigner function? These are important but rather difficult question of relevant to many problems of fundamental interest [10]. Our numerical analysis will show that the quantum dynamical manifestation of chaotic behavior does not appear on ensemble averaged oscillatory excitation numbers, but is clearly seen on the probability distributions. In Figs.3 we demonstrate moving our system from regular to chaotic dynamics by plotting the Wigner function of the system's quantum states for three values of Ω_2 : $\Omega_2/\gamma = 1$ (a), $\Omega_2/\gamma = \Omega_1/\gamma = 10.2$ (b), $\Omega_2/\gamma = 20$ (c), in a fixed moment of

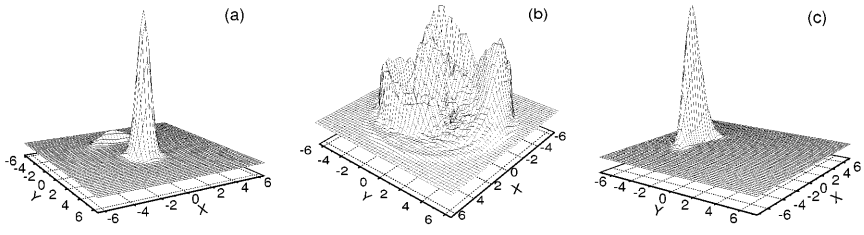

Fig. 3. Transition from regular to chaotic dynamics on the Wigner functions.The parameters are: $\chi/\gamma = 0.7$, $\Delta/\gamma = -15$, $\Omega_1/\gamma = \Omega_2/\gamma = 10.2$, $\delta/\gamma = 5$. The averaging is over 2000 trajectories.

time. The values of Δ/γ ($\Delta = \omega_0 - \omega_1$), χ/γ, and Ω_1/γ are chosen to lead to bistability in the model of single driven oscillator ($\Omega_2 = 0$).

We can see that for the case of a weak second force Fig.3(a) the Wigner function has two humps, corresponding to the lower and upper level of excitation of anharmonic oscillator in the bistability region. The hump centered close to $x = y = 0$ describes the approximately coherent lower state, while the other hump describes the excited state. The graphs in Fig.3 are given at an arbitrary time, exceeding the damping time. As calculations show, for the next time intervals during the period of modulation $t = 2\pi/\delta$, the hump corresponding to the upper level rotates around the central peak. When we increase the strength of the second force, the classical system reaches to a chaotic dynamics. The Wigner function for the chaotic dynamics is depicted in Fig.3(b). Further increasing Ω_2, the system returns to the regular dynamics. The corresponding Wigner function at an arbitrary time exceeding the transient time is presented in Fig.3(c). It contains only one hump, rotating around the centre of the phase-space within the period. As we see, the Wigner function reflecting chaotic dynamics (Fig.3(b)), has a complicated structure. Nevertheless, it is easy to observe that its contour plots in (x, y) plane are generally similar to the corresponding classical Poincaré section. Now we will consider this problem in more detail, comparing the results for contour plots with classical strange attractors on the classical maps, for the same sets of parameters. The results are shown in Fig.4.

It can be seen in Fig.4.(a) that for the deep quantum regime ($\chi/\gamma = 0.7$, $\Delta/\gamma = -15$, $\delta/\gamma = 5$), the contour plot of the Wigner function is smooth and concentrated approximately around the attractor (Fig.4(b)). Nevertheless, the different branches of the attractor are hardly resolved in Fig.4.(a). It can also be seen, that in this deep quantum regime, an enlargement of the Wigner function occurs in contrast to the Poincaré section.

Taking a smaller χ/γ, the contour plot of the Wigner function approaches the classical Poincaré section. This can be seen in Figs.4(d),(c). For the last case the correspondence is maximal, and some details of the attractor (Fig.4(d)) are resolved much better in Fig.4(c).

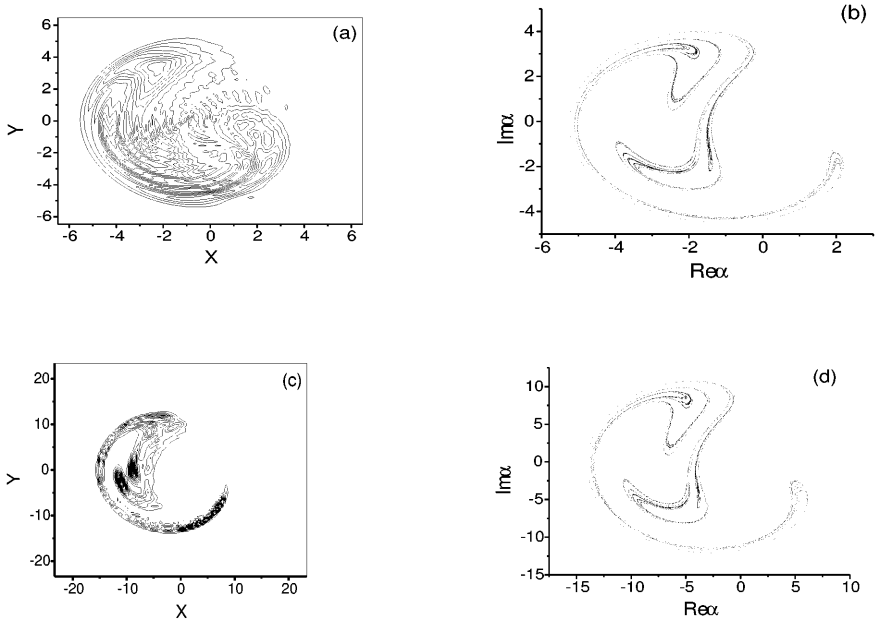

Fig. 4. Contour plot of Wigner function (a), (c) corresponding to quantum chaos and Poincaré sections (b), (d) (approximately 20000 points) for the classical complex amplitude of double driven anharmonic oscillator, plotted at times of constant phase $\delta t = 2\pi n$, $(n = 1, 2, 3, ...)$. The parameters for the cases of (a), (c) are the same as in (b), (d) respectively.

5 Conclusion

We have formulated the effective method for computation of quantum distributions based on MQSD approach to open quantum systems. Using this approach we have numerically investigated the Wigner functions for two dissipative quantum systems showing both instability and chaos in a classical limit. We have shown how quantum instability and quantum chaos are displayed on the Wigner functions.

References

[1] C. W. Gardiner, Handbook of Stochastic Methods, (Springer, Berlin, 1986); D.F. Walls and G. J. Milburn Quantum Optics (Springer, Berlin, 1996).
[2] H. Y. Carmichael, An Open System Approach to Quantum Optics, Lecture Notes in Physics (Springer-Verlag, Berlin, 1993); M. B. Plenio and P. L. Knight, Rev. Mod. Phys. **70,** 101 (1998).
[3] N. Gisin and I.C. Percival, J. Phys. A **25,** 5677 (1992); A **26,** 2233 (1993); A **26,** 2245 (1993).

[4] R. Schack, T. A. Brun, and I. C. Percival, J. Phys. A **28,** 5401 (1995).
[5] P. D. Drummond, K. J. McNeil, and D. F. Walls, Opt. Acta **27,** 321 (1980); **28,** 211 (1981).
[6] S. Schiller and R. Byer, J. Opt. Soc. Am., B **10,** 1696 (1993).
[7] S. T. Gevorkyan, G. Yu. Kryuchkyan, and N. T. Muradyan, Phys. Rev. A **61,** 043805 (2000).
[8] H.H. Adamyan, S.B. Manvelyan, and G.Yu. Kryuchkyan, Phys.Rev, A **63**, 022102 (2001).
[9] P.D. Drummond and D. Walls, J. Phys. A **13** 725 (1980).
[10] *Quantum Chaos*, Eds. G. Casati and B. Chirikov (Cambridge University Press, 1995); F. Haake, "Quantum Signatures of chaos", (Springer-Verlag, Berlin, 2000).